Journal of Power Sources 195 (2010) 4022–4029

Contents lists available at ScienceDirect

Journal of Power Sources

journal homepage: www.elsevier.com/locate/jpowsour

Pt–Ru electrocatalysts supported on ordered mesoporous carbon for direct methanol fuel cell

J.R.C. Salgado[a,1], F. Alcaide[b], G. Álvarez[b], L. Calvillo[c], M.J. Lázaro[c], E. Pastor[a,*]

[a] Dpto de Química Física, Universidad de la Laguna, Avda. Astrofísico Francisco Sánchez, 38071 - La Laguna, Santa Cruz de Tenerife, Spain
[b] Dpto de Energía, CIDETEC, P° Miramón, 196, 20009 Donostia/San Sebastián, Spain
[c] Instituto de Carboquímica, Miguel Luesma Castán 4, 50018, Zaragoza, Spain

ARTICLE INFO

Article history:
Received 8 June 2009
Received in revised form 30 October 2009
Accepted 3 January 2010
Available online 11 January 2010

Keywords:
Pt–Ru electrocatalysts
Ordered mesoporous carbon
Methanol oxidation
Direct methanol fuel cell

ABSTRACT

Pt–Ru electrocatalysts supported on ordered mesoporous carbon (CMK-3) were prepared by the formic acid method. Catalysts were characterized applying energy dispersive X-ray analyses (EDX) and X-ray diffraction (XRD). Methanol and carbon monoxide oxidation was studied electrochemically by cyclic voltammetry, and current–time curves were recorded in a methanol solution in order to establish the activity towards this reaction under potentiostatic conditions. The physicochemical and electrochemical properties of the Pt–Ru catalysts supported on CMK-3 carbon were compared with those of electrocatalysts supported on Vulcan XC-72 and commercial catalyst from E-TEK. Additionally, in order to complete this study, Pt electrocatalysts supported on CMK-3 and Vulcan XC-72 were prepared by the same method and were used as reference. Results showed that the Pt–Ru/CMK-3 catalyst presented the best electrocatalytic activity towards the CO oxidation and, therefore, good perspectives to its application in DMFC anodes. On the other hand, the activity of the Pt–Ru/CMK-3 catalyst towards methanol oxidation was higher than that of the commercial Pt–Ru/C (E-TEK) catalyst on all examined potentials, confirming the potential of the bimetallic catalysts supported on mesoporous carbons.

1. Introduction

Direct methanol fuel cells (DMFC) have attracted much attention due to their potential applications as clean and portable power sources, and additionally, because of the advantages of the use of a liquid fuel [1–4]. However, various issues such as poor kinetics of methanol oxidation, methanol crossover through the membrane, low electrocatalytic activity and durability of the electrocatalysts still remain as key problems for the commercialization of DMFC [5–20].

To improve the electrocatalytic activity of methanol electro-oxidation, many efforts have been devoted towards the development of electrocatalysts [6–19]. Pt anodes are rapidly poisoned in DMFC due to strong CO adsorption on the metal surface, leading to a significant decrease in power output of the cell [5]. Consequently, Pt could never be good electrocatalysts for methanol electro-oxidation at room temperature. In this sense, various Pt-based alloys have also been investigated [10–18]. At the moment, Pt–Ru alloy electrocatalysts are generally regarded as the most appropriate material for methanol electro-oxidation due to their tolerance towards CO [6–9]. Ru forms oxygenated species at lower potential than Pt and its presence in the electrocatalysts promotes oxidation of CO into CO_2 by the bifunctional mechanism and/or a "ligand effect" [9,20,21].

The maximum utilization of the Pt–Ru electrocatalysts particles by choosing the proper supporting material would improve the performance of DMFC [22–45]. The ideal support material should have some specific characteristics: high electrical conductivity, adequate metal–support interactions at the electrode and also good corrosion resistance under oxidizing conditions. Carbon black is the most common support material for metals at the electrode in fuel cells [14–17,19,22]. Nowadays, alternative carbon materials such as carbon or graphite nanofibers [30–32], carbon nanotubes [33–36] and mesoporous carbons [37–45] have been investigated as supports for the development of DMFC.

From these results it could be expected that the electrocatalysts supported on these non-conventional carbon materials would show a better performance for methanol electro-oxidation than commercial ones. The ordered mesoporous carbons (OMC) have received great attention because of their potential use as electrocatalytic supports in fuel cell electrodes since the discovery of the mesoporous silica materials. However, the mesoporous carbon contains a small amount of oxygen surface groups, which can be disadvantageous for many applications.

* Corresponding author. Tel.: +34 922 319071; fax: +34 922 318002.
E-mail address: epastor@ull.es (E. Pastor).
[1] Present Address: Instituto Superior Técnico, Instituto de Ciência e Engenharia de Materiais e Superfície, Av. Rovisco Pais 1049-001, Lisboa, Portugal.

0378-7753/$ – see front matter © 2010 Elsevier B.V. All rights reserved.
doi:10.1016/j.jpowsour.2010.01.001

Many works about the effect of the functionalization of the support on the preparation of catalysts can be found in the literature. However, the effect of the functionalization on the properties of catalysts has not been well established, due to they not only depend on the functionalization of the support but also on the textural and morphological properties of the support [46], the catalyst preparation method and the nature of the metal precursor [47,48]. The results obtained in these works indicate that the oxidation treatments affect drastically the properties of both the carbons and the catalysts prepared on them. Some authors have found that the interaction of the metal precursor with the carbon support, by means of surface oxygen groups, leads to a higher dispersion [46,49]. However, other studies have shown that the oxidation of the support has a negative effect on getting a catalyst with a high dispersion [50,51].

In recent studies of our group, Pt nanoparticles were deposited by the formic acid and borohydride reduction methods on ordered mesoporous carbons CMK-3 subjected to different chemical treatments [37,38]. We found that a good dispersion of the electrocatalysts on the support was achieved and showed that CO-stripping occurs at more negative potentials (around 0.15 V) with these supports respect to Vulcan XC-72. The best results were obtained with CMK-3 functionalized with concentrated nitric acid during 0.5 h, which is the support with the highest content of surface oxygen groups maintaining the ordered structure. According to this previous result, this treatment was chosen for the preparation of the materials in the present paper.

In the present work, OMC supported Pt–Ru electrocatalysts was prepared applying the formic acid reduction method (FAM) and the oxidation of methanol and carbon monoxide were investigated. Its electrochemical properties were compared with those for Pt–Ru electrocatalyst supported on a commercial carbon substrate (Vulcan XC-72) and a commercial Pt–Ru/C catalyst from E-TEK. In order to complete this study, results were also compared with those for Pt electrocatalysts supported on CMK-3 and Vulcan XC-72, which were prepared by the same method. All materials were characterized applying energy dispersive X-ray analyses (EDX) and X-ray diffraction (XRD). Methanol and carbon monoxide oxidation was studied electrochemically by cyclic voltammetry. Current–time curves were recorded in a methanol solution in order to establish the activity towards this reaction under potentiostatic conditions.

2. Experimental methods

2.1. Synthesis and functionalization of carbon supports

Ordered mesoporous carbon CMK-3 was synthesized by incipient wetness impregnation of SBA-15 silica as described in [52]. In a typical synthesis, SBA-15 silica was impregnated with a carbon precursor (polymerized furan resin). Impregnated silica was cured at 108 °C for 24 h and carbonized at 700 °C for 3 h. The obtained silica-carbon composite was washed with NaOH to remove the SBA-15 silica. Subsequently, CMK-3 carbon was refluxed in concentrated HNO_3 at room temperature for 0.5 h to modify its surface chemistry. Surface oxygen groups were created during this treatment and the ordered structure of the original CMK-3 carbon was maintained.

Carbon Vulcan XC-72, supplied by Cabot, was also used as electrocatalyst support for comparison.

Carbon supports (CMK-3 and Vulcan XC-72) were characterized by different analytical techniques (XRD, N_2-physisorption and TPD experiments) in order to study their morphological and textural properties as well as their surface chemistry [52]. These properties will be related to the physicochemical and electrochemical properties of the catalysts.

2.2. Preparation of the carbon-supported Pt and Pt–Ru electrocatalysts

The mesoporous carbon-supported Pt and Pt–Ru electrocatalysts (denoted as Pt/CMK-3 and Pt–Ru/CMK-3) were prepared by the formic acid method (FAM) [26,27,38]. The method consists of the following steps: first, the formic acid solution was added to the carbon material at 80 °C. Then, chloroplatinic acid ($H_2PtCl_6{\cdot}6H_2O$, Johnson Matthey) solution was slowly dropped under sonication to obtain a good dispersion of Pt/C. In the case of Pt–Ru/CMK-3, the procedure is similar, with the exception that a solution containing both metal precursors ($H_2PtCl_6{\cdot}6H_2O$ and $RuCl_3$, Johnson Matthey) is employed.

Appropriate concentrations of the precursors were used to obtain a theoretical *total* metal loading of 20 wt.% and a Pt:Ru composition of 50:50.

The same procedure was used for preparing Pt and Pt–Ru catalysts supported on Vulcan XC-72 (denoted as Pt/Vulcan and Pt–Ru/Vulcan).

2.3. Physicochemical characterization of Pt/C and Pt–Ru/C electrocatalysts

The real content of Pt and Pt–Ru in the electrocatalysts and the Pt to Ru ratio were determined by energy dispersive X-ray analyses (EDX) technique coupled to a scanning electron microscopy Jeol JEM Mod. 1010 with a silicon detector with Be window and applying 20 keV.

X-ray diffractograms of the electrocatalysts were obtained in a universal diffractometer Carl Zeiss-Jena, URD-6, operating with Cu Kα radiation (λ = 0.15406 nm) generated at 45 kV and 40 mA. Scans were done at 3° min^{-1} for 2θ values between 0° and 100°. In order to estimate the crystallite size from XRD Scherrer's equation was used [53] and the (2 2 0) peak of the Pt fcc structure around 2θ = 70° was selected. This region was choosen to avoid the influence of a broad band of the carbon substrate (2θ = 25°) on the (1 1 1) and (2 0 0) peaks of Pt structure [25,54]. The lattice parameters were obtained by refining the unit cell dimensions by the least squares method [55].

2.4. Electrochemical characterization of Pt/C and Pt–Ru/C electrocatalysts

Electrochemical experiments were performed in a typical one-compartment three-electrode glass cell using a potentiostat Autolab PGSTAT302 (Ecochemie). The counter electrode was a large area pyrolitic graphite foil and the reference electrode was a reversible hydrogen electrode (RHE) placed inside a Luggin capillary. All potentials in the text are referred to this electrode. The working electrodes were prepared depositing a thin-layer of the electrocatalyst over a pyrolitic graphite disk (5 mm diameter, 0.196 cm^2 geometric area). A catalyst ink was prepared by mixing the catalyst (4.0 mg ml^{-1}), and 30 μl of Nafion dispersion (5 wt.%, Aldrich) in ultrapure water (Millipore Milli-Q system). The suspension was submitted under sonication for 10 min. An aliquot of the suspension was pipetted onto the graphite disk and dried at room temperature. After that, the working electrode was immersed into 0.5 M H_2SO_4 electrolyte solution, prepared from high purity reagents (Merck) and deaerated with argon (99.998%, Air Liquide).

Electrochemical experiments were done at room temperature. However, in the experiments performed at different temperatures to obtain the Arrhenius type plots, the reference electrode was immersed in a 0.5 M H_2SO_4 aqueous solution, thermostated at 25.0 °C in a separated compartment. In this case, the latter was connected to the working compartment by means of a Luggin capillary.

Table 1
Estimation of the type and number of surface oxygen groups obtained from the deconvolution of the TPD profiles.

Support	CO_2 peak areas (μmol g^{-1})			CO peak areas (μmol g^{-1})	
	Carboxylic	Anhydride/lactone	Anhydride	Phenol	Quinone
CMK-3	1342	537	519	2471	801
Vulcan XC-72	0	0	0	0	317

Electrochemical active areas of catalysts were measured from CO-stripping voltammograms by the integration of the CO_{ad} oxidation region, assuming a charge of 420 μC cm^{-2} involved in the oxidation of a monolayer of linearly adsorbed CO. This electroactive area has been used to calculate the current densities given in the text. CO (99.997%, Air Liquide) was adsorbed on catalyst surfaces by bubbling this gas at 1atm through the electrolyte for 25 min while holding the potential at 0.20 V. The excess CO was then flushed from the electrolyte with Ar gas for 25 min and the potential was cycled between 0.05 and 0.80 or 1.10 V at 0.020 V s^{-1} for two complete oxidation/reduction scans. The first sweep was in the positive direction.

Methanol oxidation reaction was characterized by cyclic voltammetry and chronoamperometry. Cyclic voltammograms (CVs) recorded in 0.5 M H_2SO_4 + 0.50 M between 0.20 and 0.80 V for Pt–Ru/C and 1.10 V for Pt/C at a scan rate of 0.02 V s^{-1}. The upper limit potential for Pt–Ru/C electrocatalysts was restricted to 0.80 V, since the application of higher values induces irreversible changes in the particle surface composition with the increase of Pt concentration due to Ru dissolution [28]. Potentiostatic *j*–*t* curves were recorded in the same solution at 0.60 V for 900 s, unless other conditions will be specified in the text.

3. Results and discussion

3.1. Physicochemical characterization of the supports and electrocatalysts

Carbon materials used as support presented different properties that will influence the final properties of the catalysts and their electrocatalytic activity. The physicochemical characterization of the CMK-3 carbon was stated in a previous work [52]. CMK-3 carbon structure consisted of periodic arrays of carbon nanorods with uniform mesopores between them. This structure was maintained after the HNO_3 treatment. On the other hand, Vulcan XC-72 consisted of an aggregation of spherical carbon nanoparticles, called primary particles.

Textural properties of the carbon supports were determined by N_2-physisorption. CMK-3 carbon had a specific surface area of around 400 m^2 g^{-1} and a total pore volume of 0.27 cm^3 g^{-1}. This material was mainly a mesoporous carbon, although it contained a small amount of micropores. However, Vulcan XC-72, that had a specific surface area of 218 m^2 g^{-1} and a total pore volume of 0.41 cm^3 g^{-1}, contained a considerable amount of micropores (30% of total surface area). The presence of microporous could result in a lower electrochemical activity due to the less efficient diffusion of reactants and products.

Finally, the surface chemistry of the carbon materials was studied by temperature-programmed desorption experiments [52]. It has been proved that the presence of functional groups on the carbon surface influences the properties of the catalyst [46,49,51]. Table 1 shows an estimation of the type and number of the surface groups. It can be observed that CMK-3 carbon contains a great number of surface oxygen groups compared to Vulcan XC-72. CMK-3 carbon has mainly carboxylic and phenol groups, whereas Vulcan XC-72 only contains a small amount of quinones.

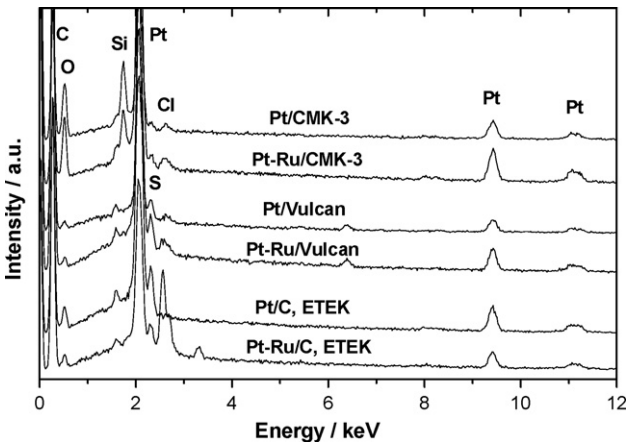

Fig. 1. EDX spectrum of the Pt and Pt–Ru electrocatalysts supported on CMK-3 and Vulcan XC-72 and compared with E-TEK materials.

EDX spectra of the electrocatalysts prepared by FAM using CMK-3 and Vulcan XC-72 as carbon supports, compared with those for commercial E-TEK materials are given in Fig. 1. The analysis showed the presence of Pt, C, S, O and Cl for all materials. Cl-atoms proceed from the precursor salts used for the preparation of the catalysts. It is remarkable that for CMK-3 electrocatalysts the amount of O is the highest due to the introduction of the oxygen groups previously mentioned, whereas the content of S in this type of carbon support is negligible. In this case, Si from the silica used as template for the preparation of the OCMs is also present in the spectra. It has been reported that the presence of this Si does not affect the electrochemical response [37,38].

The values of the metal content obtained for Pt/C and Pt–Ru/C electrocatalysts from EDX are similar to the nominal value of 20% (Table 2). Finally, it was found that the EDX atomic composition was 85:15 for Pt:Ru supported on CMK-3 and Vulcan XC-72, and 50:50 for E-TEK catalysts, respectively, as shown in Table 2. The low content of Ru obtained with the FAM procedure has been previously described in the literature and depends on the pH of the formic acid solution [56].

X-ray diffractograms for Pt/C and Pt–Ru/C electrocatalysts can be seen in Fig. 2. A broad peak at around $2\theta = 25^\circ$ was observed in all diffractograms that is associated with the carbon support material. This peak is assigned to the basal planes of graphite (0 0 2) and was more intense in catalysts supported on Vulcan XC-72. In the case of Vulcan XC-72, this peak is attributed to the turbostratic structure of the primary particles, which consist of "crystalline" regions of 1.5–2.0 nm in length and 1.2–1.5 nm in height with a random disposition. However, CMK-3 carbon shows a broader peak of low intensity, indicating that it was an amorphous carbon material. The nature of the carbon support affects the supported metal particles, as will be seen below.

The crystalline structure of the metal in the nanoparticles is evident and all the XRD patterns clearly show the five main charac-

Table 2
Ru content from EDX and physical characteristics from XRD analysis of the carbon-supported Pt and Pt–Ru electrocatalysts.

Electrocatalyst	Pt:Ru	% Pt	*d* (nm)	Lattice parameter (Å)	Metal surface area (m^2 g^{-1})
Pt/CMK-3	–	18	4.5	3.9132	62
Pt–Ru/CMK-3	85:15	15	3.2	3.9179	94
Pt/Vulcan	–	14	2.8	3.9214	100
Pt–Ru/Vulcan	85:15	20	2.9	3.9125	103
Pt/C, E-TEK	–	16	2.8	3.9231	100
Pt–Ru/C, E-TEK	50:50	20	3.4	3.8775	105

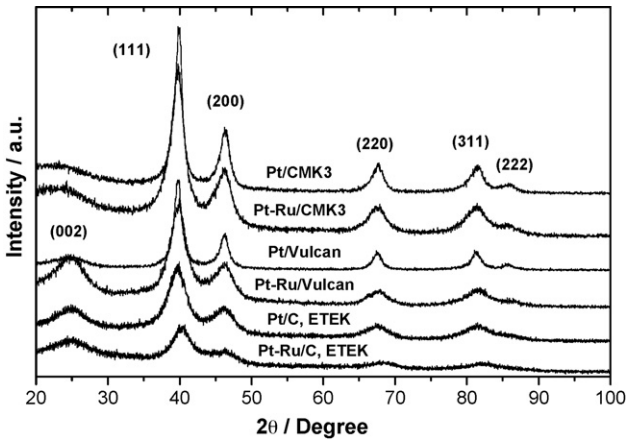

Fig. 2. XRD diffractograms of the Pt and Pt–Ru electrocatalysts supported on CMK-3 and Vulcan XC-72 and compared with E-TEK materials.

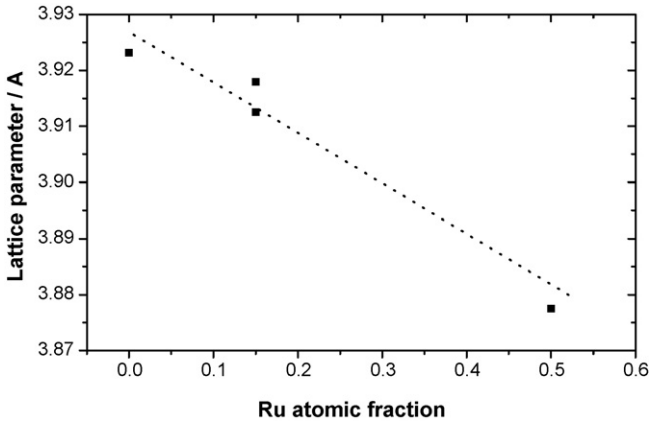

Fig. 3. Dependence of the lattice parameter on Ru atomic fraction.

teristic peaks of the face centred cubic (fcc) crystalline Pt, namely, the planes (1 1 1), (2 0 0), (2 2 0), (3 1 1), and (2 2 2). No peaks corresponding to a metallic ruthenium with a hexagonal close packed (hcp) structure or the ruthenium oxide phase were observed [28]. These results suggest that for the materials prepared in the present paper, Ru is incorporated in the Pt fcc structure. However, it is possible that metallic Ru is not detected because the intensities of its reflections are much smaller than those of the Pt. In fact, Chu and Gilman suggested [11] that the presence of hcp structures of Pt–Ru bimetallic materials are observed only when the percentage of Ru is above 50 at.%.

The diffraction peaks in the Pt–Ru/C electrocatalysts are slightly shifted to higher 2θ values with respect to the same reflections in Pt/C and show the effect of increasing amounts of Ru in the electrocatalysts. This is a consequence of the incorporation of Ru in the fcc structure of platinum and suggests the formation of a Pt–Ru/C alloy in the electrocatalysts [11,12].

The lattice parameter was calculated from the XRD in Fig. 2, considering the peak position for Pt signals and the results are summarized in Table 2. The value for Pt–Ru/Vulcan electrocatalyst (3.9125 Å) is lower than that of Pt/Vulcan electrocatalyst (3.9214 Å) and the same occurs for E-TEK materials, indicating a contraction of the lattice due to the Pt–Ru alloying to some extent [11]. In the studies of Chu and Gilman on the preparation of a wide compositional range of unsupported Pt–Ru alloy electrocatalysts by thermal decomposition of chlorides and chloroacids, a decrease of the lattice parameter due to incorporation of Ru-atoms in the fcc structure of Pt was found [11]. The authors showed that in all cases Ru was alloyed with Pt. Accordingly, the decrease observed for the lattice parameter in the present paper corroborates the formation of a Pt–Ru alloy in the electrocatalysts [11,12]. The allowing of all the materials studied is confirmed by the linear relationship found between the lattice parameter and the Ru atomic fraction, following the Vegard's law (Fig. 3). It is remarkable that the value of the lattice parameter for Pt/CMK-3 is smaller than expected and does not match the previous arguments, but as shown in [38], follows the general behaviour observed for the Pt materials prepared with the FAM method.

On the other hand, there is a second factor which affects the lattice parameter that is the crystallite size. The dependence of the lattice parameter on the crystallite size for the electrocatalysts prepared by formic acid and borohydride methods has been described previously [15–17,27,38]. It was observed that the increase in the crystallite size for CMK-3 supported Pt electrocatalysts produces a diminution in the lattice parameter, effect which is more apparent when the FAM method is used [38]. Accordingly, the lattice parameter for Pt–Ru/CMK-3 (3.9190 Å) is higher than for Pt–Ru/Vulcan (3.9125 Å), as the former presents a crystallite size of 3.2 nm whereas the latter is 2.9 nm for the same Pt–Ru composition, i.e. an expansion of the lattice of Pt occurs, due to the increase in the crystallite size for these Pt–Ru materials.

As can be observed in Fig. 2, the intensity and width of the peaks, which are related with the metal crystallite size, depended on the carbon material used as support. The diffraction peaks of the electrocatalysts supported on CMK-3 material were sharper than those on Vulcan XC-72 carbon, indicating larger metal crystallites. Taking into account that all catalysts were prepared by the same method and with similar metal loading, it is deduced that the support affects the size of supported metal crystallites. Mean metal crystallite sizes for the electrocatalysts, calculated from the Scherrer' equation, are given in Table 2. The crystallite sizes for Pt–Ru/C and Pt/C electrocatalysts were similar in the range of 2.8–3.4 nm with the exception of Pt/CMK-3 (4.5 nm). However, a relationship between the metal crystallite size and the crystalline grade of the support can be established, as has been already observed by other authors [57,58]. The higher the crystalline grade of the support, the smaller the metal crystallite size. In the literature, this effect is attributed to the type of metal–support interaction [57,58]. It is remarkable that the crystalline structure of the metal is clearly visible in the nanoparticles and that the crystallite size is similar in the cases for Vulcan XC-72 and E-TEK samples, as expected [27,38].

The surface area (SA) was calculated (Table 2) applying the equation $SA\ (m^2\ g^{-1}) = 6 \times 10^3/\rho d$, where d is the mean metal crystallite size in nm and ρ is the density of Pt or Pt–Ru considering $\rho_{Pt-Ru}\ (g\ cm^{-3}) = \rho_{Pt}X_{Pt} + \rho_{Ru}X_{Ru}$, where ρ_{Pt} of Pt metal is 21.4 g cm^{-3} and ρ_{Ru} is 12.3 g cm^{-3}, and X_{Pt} and X_{Ru} are the weight percent of Pt and Ru, respectively, in the catalysts. Values around 100 m^2 g^{-1} were obtained for all catalysts with the exception of Pt/CMK-3, which is lower as expected from its higher crystallite size.

3.2. Electrochemical studies

3.2.1. Carbon monoxide oxidation

CO-stripping voltammetry can be used to obtain some in situ information about composition and surface areas of catalysts, as well as, to establish their tolerance towards CO poisoning. In Fig. 4, CO-stripping voltammograms at room temperature are shown for Pt and Pt–Ru based catalysts. In addition, the second cycles recorded after CO-stripping which correspond to the voltammograms in the base electrolyte for the clean surfaces are shown. The CO_{ads} oxidation peak potentials on Pt/Vulcan and Pt/E-TEK catalysts are observed around 0.82 V. For Pt/CMK-3 catalyst the CO_{ads} oxidation

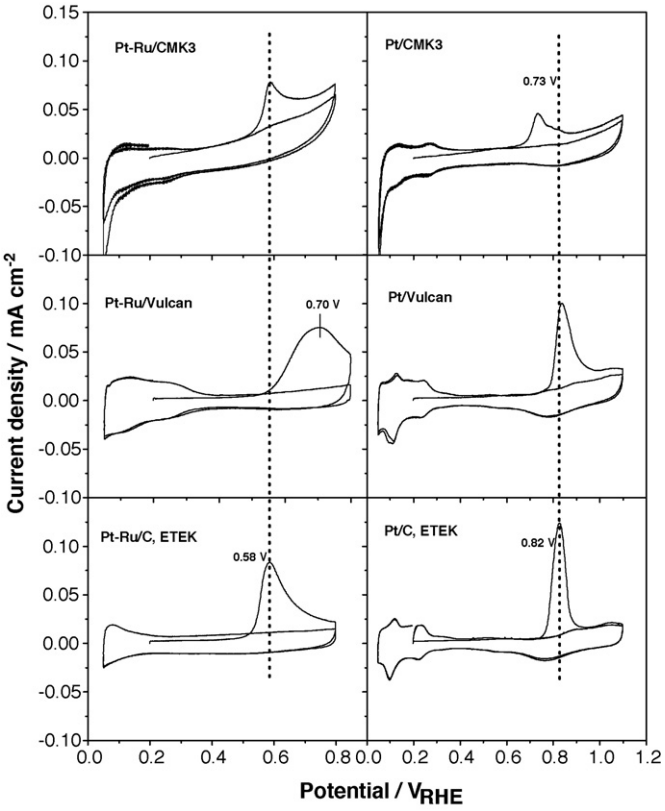

Fig. 4. CO-stripping voltammetries for Pt/C and Pt–Ru/C electrocatalysts in 0.5 M H_2SO_4. E_{ad} = 0.20 V; ν = 20 mV s^{-1}; T = 25 °C.

peak potential appears at 0.73 V. This shift to more negative values could suggest an effect of the carbon support and it indicates faster charge transfer kinetics of the CO oxidation process [14].

The onset potential of CO oxidation is shifted negatively for the three Pt–Ru based catalysts, with respect to that of the Pt-based catalysts. This fact could be explained by the presence of Ru, which is more easily electro-oxidized than pure Pt, and forms $Ru–OH_{ads}$ species at lower potentials, helping to oxidize the CO_{ads}, through a bifunctional mechanism [7,21]. The CO_{ads} oxidation peak potentials on Pt–Ru/Vulcan and Pt–Ru/C (E-TEK) catalysts are attained at 0.70 and 0.58 V, respectively. The same last peak potential, and similar current, was showed by the Pt–Ru/CMK-3 catalyst. The shift to more positive potentials for the Pt–Ru/Vulcan with respect to the E-TEK material is justified by the lower Ru content of this material. Then, the comparison of the Pt–Ru/CMK-3 has to be done with the Pt–Ru/Vulcan with the same Pt:Ru composition: a shift of 0.12 V to more negative potentials is established. Taking into account the ruthenium content of Pt–Ru/CMK-3 and Pt–Ru/C (E-TEK), 15 and 50 a/o, respectively, it can be concluded that the former catalyst show the best electrocatalytic activity towards the CO oxidation, and good perspectives to its application in DMFC anodes.

3.2.2. Methanol oxidation

Fig. 5 illustrated cyclic voltammograms recorded at room temperature for Pt–Ru/CMK-3, Pt–Ru/Vulcan and commercial Pt–Ru/C (E-TEK) catalysts in 0.5 M CH_3OH + 0.5 M H_2SO_4 solution. Also reported are the cyclic voltammograms for the Pt/CMK-3, the Pt/Vulcan and the commercial Pt/C (E-TEK) catalysts in the same solution.

All the voltammograms corresponding to the catalysts based on Pt exhibit the irreversible nature of the methanol electro-oxidation. The onset of methanol electro-oxidation occurs between 0.50 and 0.62 V for the three catalysts based on Pt. The highest current densities are achieved by the Pt/CMK-3 during the positive potential scan at potentials around 0.87 V. But it is also observed that in the same potential scan direction, this catalyst presents the lowest activity for oxidation of methanol when compared with the other two catalysts at potentials lower than 0.70 V. The specific activities of the mesoporous and Vulcan carbon samples at 0.60 V vs. RHE are showed in Table 3. The current density of the methanol oxidation for Pt/CMK-3 reached a value of 21 μA cm^{-2}, which is lower than that of Pt/Vulcan (30 μA cm^{-2}) and Pt/C (E-TEK) (41 μA cm^{-2}). The data show that the Pt supported on the conventional Vulcan carbon (E-TEK) exhibits two times higher specific activity than that supported on the mesoporous carbons. This result could be attributed to the higher utilization of the Pt nanoparticles on conventional Vulcan carbon, taking into account that the size of Pt crystallites supported on conventional Vulcan carbon is about one half of that of the crystallites supported on OMC. However, it is valuable that the Pt/CMK-3 catalyst is at least comparable to a commercial catalyst, given that it has a lower surface area. Moreover, values are quite small and it can be concluded that similar results are obtained for the three materials at E < 0.70 V.

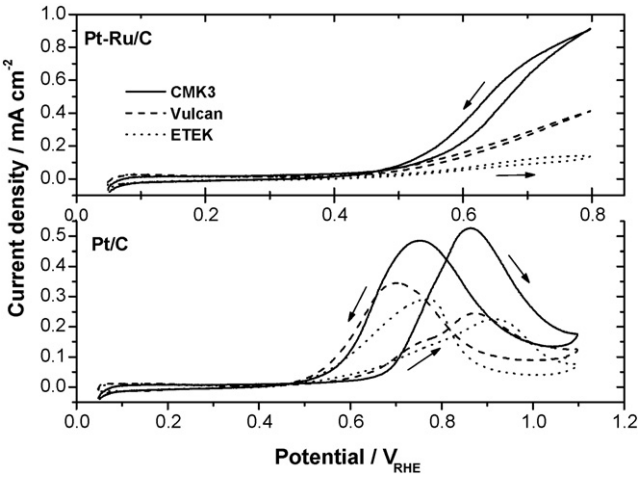

Fig. 5. Cyclic voltammograms for Pt/C and Pt–Ru/C electrocatalysts in 0.5 M CH_3OH + 0.5 M H_2SO_4. ν = 20 mV s^{-1}; T = 25 °C.

In contrast to the behaviour described above for the Pt-based catalysts, the onset potential of methanol electro-oxidation basically occurs at the same potential (≈0.40 V) for the three catalysts based on Pt–Ru. In addition, the methanol oxidation current grows considerably faster for Pt–Ru/CMK-3 catalyst as compared to the commercial Pt–Ru/C (E-TEK) one. For example, it can be found that Pt–Ru/CMK-3 catalyst displays about 4.6-fold larger methanol oxidation specific current than commercial Pt–Ru/C (E-TEK), at 0.60 V (see Table 3). Furthermore, a 1.7-fold current increase is approximately registered for the Pt–Ru/CMK-3 catalyst with respect to Pt–Ru/Vulcan prepared in the same condition as the mesoporous carbon-supported catalyst. Thus, such increase in activity may be attributed only to the supporting effect of the mesoporous carbon, because the atomic ratio Pt:Ru is the same in both catalysts,

Table 3
Current densities from cyclic voltammetric (CV) and chronoamperometric (CR) curves obtained at 0.60 V for carbon-supported Pt and Pt–Ru electrocatalysts.

Electrocatalyst	$CV_{0.60}$ (μA cm^{-2})	$CR_{0.60}$ (μA cm^{-2})
Pt/CMK-3	21	8
Pt–Ru/CMK-3	223	102
Pt/Vulcan	30	23
Pt–Ru/Vulcan	134	91
Pt/C, E-TEK	41	35
Pt–Ru/C, E-TEK	48	74

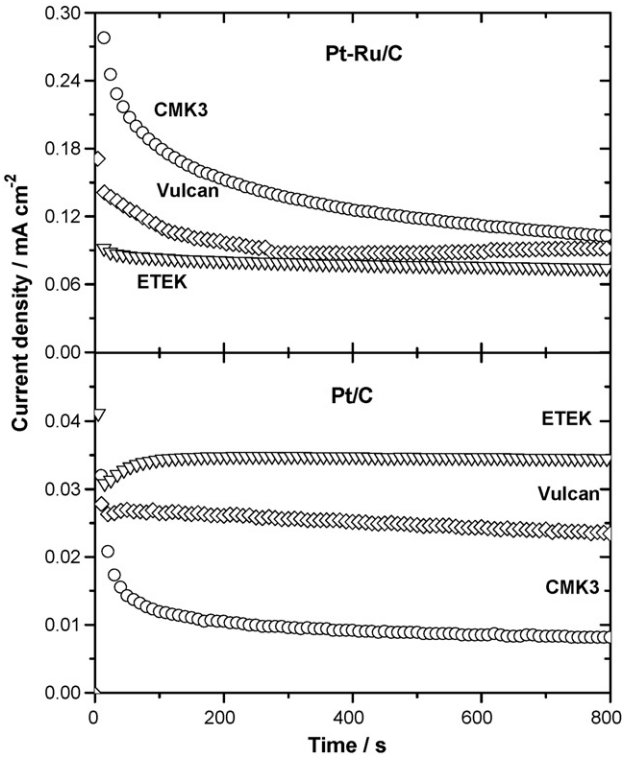

Fig. 6. Chronoamperometric curves recorded in a 0.5 M CH_3OH + 0.5 M H_2SO_4 solution at E = 0.60 V.

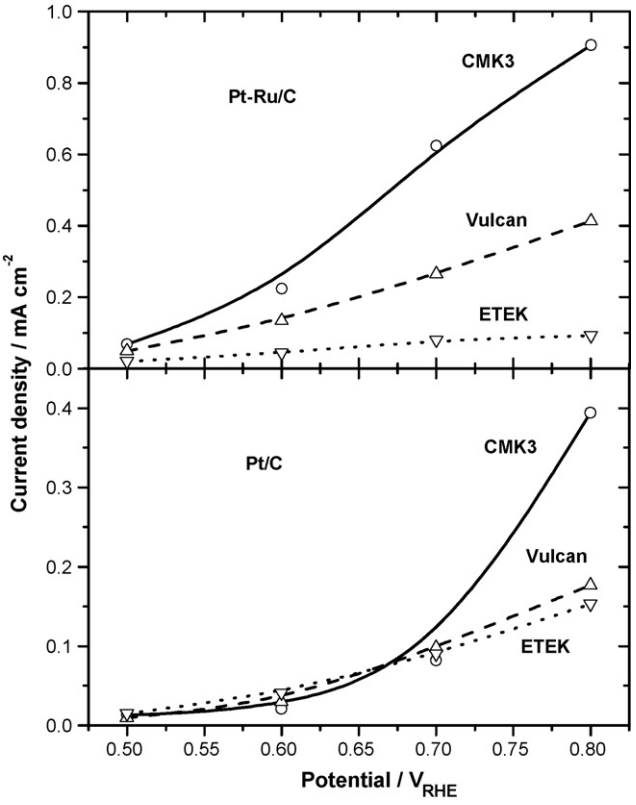

Fig. 7. Current densities at potentials in the range 0.50–0.80 V obtained in a 0.5 M CH_3OH + 0.5 M H_2SO_4 solution.

and there is not a significant difference between the crystallite sizes of both materials, as can be seen in Table 2. Taking into account that an improvement of the methanol electro-oxidation was not observed for Pt/CMK-3, although the oxygen groups of the support facilitate the CO oxidation (see Fig. 4), it may be conclude that the support has an effect on the Pt–Ru interactions that improves the methanol deprotonation. These results confirm that the catalyst Pt–Ru/CMK-3 is notably more active for electrooxidizing methanol than commercial catalysts commonly employed as anodes in DMFCs.

Interestingly, the Pt–Ru/Vulcan catalyst showed higher oxidation activity than those of the PtRu/C (E-TEK) catalyst also supported on the Vulcan carbon. This improved methanol reaction rate observed could be due to the catalyst preparation procedure, but also could in part be connected to a different Pt:Ru ratio with respect to the Pt–Ru/C (E-TEK) catalyst. In this sense, Gasteiger et al. [59] investigated the effect of surface composition of well-defined Pt–Ru "bulk" alloy catalysts on methanol electro-oxidation. They showed that a maximum in the current density was found for Pt–Ru alloys with a Ru content between 7 and 33 a/o, as the temperature was increased from 25 to 60–80 °C. Later on, reasonably similar results for Pt–Ru alloys were also described by other researchers [60,61]. As pointed out above, the Ru atomic ratio in Pt–Ru/Vulcan is 15 a/o, i.e. lower than in the Pt–Ru/C (E-TEK) catalyst (50 a/o), but the same as Pt–Ru/CMK-3. Then, it seems reasonable that the decrease in the Ru content in Pt–Ru/Vulcan catalyst contributes to the observed increased intrinsic activity as compared to Pt–Ru/C (E-TEK).

To further assess steady-state catalyst performance with respect to methanol electro-oxidation we have carried out chronoamperometry tests at steady potential. Fig. 6 shows the potentiostatic methanol oxidation currents, normalized by the active surface area of the catalysts, as a function of time for the Pt and Pt–Ru based catalysts at 0.60 V. Generally, the curves feature a sharper decrease during the earlier minutes. Afterwards, the current diminishes much more slowly. This behaviour has been ascribed to the accumulation of poisoning species, mainly CO, on the Pt surface during the methanol oxidation or, in turn, to the formation of Ru oxides as the cause of the initial rapid decay [62]. The subsequent slow current decrease could be tentatively ascribed to the presence of surface active impurities or anions in the electrolyte solution that may slowly adsorb onto the catalyst surface during long-term experiments, thereby determining loss of activity [63,64].

It is apparent from the slopes of the current decaying region in Fig. 6, that the rate of deactivation due to the poisoning species is less for the Pt/Vulcan and Pt/C (E-TEK) catalysts than for the Pt/CMK-3 catalyst, suggesting a better tolerance towards poisoning of the Pt-on-Vulcan catalysts than Pt-on-CMK-3. A reason could be the better water adsorption capability of the Vulcan carbon compared to that of the mesoporous carbon [65]. Quasi-stationary current densities from chronoamperometric curves increased in the order Pt/CMK-3 < Pt/Vulcan < Pt/C (E-TEK) as can be seen in Table 3.

Regarding to the Pt–Ru based catalysts, Pt–Ru/CMK-3 displays the highest activity followed by Pt–Ru/Vulcan, and Pt–Ru/C (E-TEK). It appears that the greater activity of Pt–Ru/CMK-3 compared to Pt–Ru/C (E-TEK) is due to the effect of carbon support, because both catalyst had the same Pt:Ru atomic ratio and the crystallite sizes are very similar. On the other hand, the differences between Pt:Ru atomic ratio could explain the higher activity of Pt–Ru/Vulcan than Pt–Ru/C (E-TEK) catalyst. As we stated above, other authors have addressed methanol oxidation activity of bulk Pt–Ru alloy electrocatalysts as a function of Pt:Ru ratio using chronoamperometric methods [63]. They found increasing activity at room temperature as platinum content grew from about 50 up to somewhere between 67 and 93 a/o, and they ascribed this behaviour to an increased ability of the Pt-rich alloys to promote the adsorption and initial dehydrogenation of methanol.

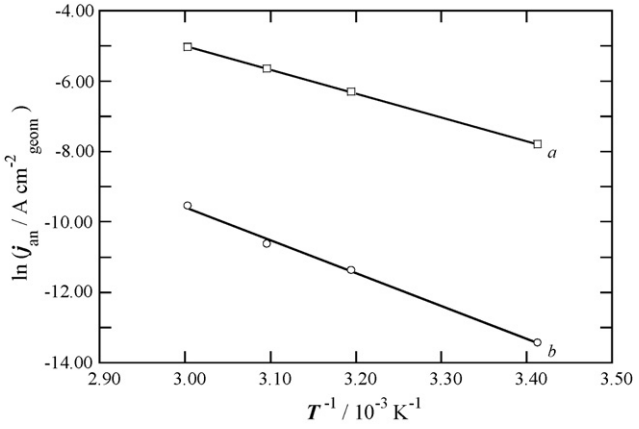

Fig. 8. Arrhenius plot of methanol electro-oxidation on (a) Pt–Ru/CMK-3 and (b) Pt/CMK-3 catalysts taken in a 2.0 M CH_3OH + 0.5 M H_2SO_4 solution at 0.50 V.

Fig. 7 allows to compare the resulting activities obtained from cyclic voltammograms in Fig. 5 for Pt and Pt–Ru based catalysts at the more technically interesting potentials of the methanol oxidation reaction. The activity of the Pt–Ru/CMK-3 catalyst towards methanol oxidation is higher than that of the commercial Pt–Ru/C (E-TEK) catalyst on all examined potentials, confirming the potential of the bimetallic catalysts supported on mesoporous carbons.

The influence of temperature on the kinetics of methanol oxidation reaction on both Pt/CMK-3 and PtRu/CMK-3 catalysts was investigated by performing chronoamperometric curves at the steady potential of 0.50 V in 2.0 M CH_3OH in 0.50 M H_2SO_4, in the range of 20.0–60.0 °C. The form of the *j*–*t* curves (not shown) at different temperatures was essentially the same as those in Fig. 6.

Activation energy provides important information for both the elucidation of fundamental catalytic mechanisms and the projection of actual fuel cell performance. Therefore, current density values were taken at 800 s in order to evaluate apparent activation energies, and the corresponding ln(*j*) *vs.* T^{-1} (Arrhenius type) plots were obtained (see Fig. 8). Good straight lines with linear regression coefficient $r \geq 0.999$ were always found. Plots of Fig. 8 allow to determine the apparent activation energy at 0.50 V, $U^{\#}_{app}(0.50\,V)$, since the slope of Arrhenius type plots can be taken as $-U^{\#}_{app}(E)/R$ [66], where *R* is the gas constant (=8.314 J K^{-1} mol^{-1}). The apparent activation energies for methanol oxidation on Pt/CMK-3 and Pt–Ru/CMK-3 catalysts were 77.4 and 56.2 kJ mol^{-1}, respectively. These values are comparable with those previously reported in the literature [63,67–69]. Therefore, it can be concluded that the carbon support has not a significant effect on the activation energy, so it is expected that the effect of the temperature on the electrocatalytic performance of the catalysts supported on OMC will be similar to that described in the literature.

4. Conclusions

The main conclusions derived from this work can be summarized as follows:

- The size of metal crystallites depends on the nature of the support. The higher the crystalline grade of the support, the smaller the metal crystallite size. This effect is associated with the electronic metal–support interaction, which increases with the crystalline grade of the support.
- Pt and $Pt_{85}Ru_{15}$ electrocatalysts supported on ordered mesoporous carbon (CMK-3) show more negative CO oxidation potential as well as higher catalytic efficiency for oxidation of methanol compared with catalysts supported on Vulcan XC-72 (and also commercial catalysts from E-TEK). The increase in the activity is attributed to the supporting effect of the mesoporous carbon, as metal loading are similar for all catalysts and the Pt:Ru atomic ratio is the same for prepared bimetallic materials.
- Carbon support has not a significant effect on the activation energy. Therefore, the effect of the temperature on the electrocatalytic performance of the catalysts supported on OMC will be similar to that described in the literature for Vulcan catalysts.

These results prove the potential of bimetallic catalyst supported on ordered mesoporous materials for their use in DMFC anodes.

Acknowledgements

The authors gratefully acknowledge financial support given by the Spanish MEC under the projects MAT2008-06631-C03-01, 02 and 03 (FEDER). L. Calvillo and J.R.C. Salgado (BES-2005-0169) thank MEC for the predoctoral and postdoctoral fellowship, respectively.

References

[1] W. Vielstich, H.A. Gasteiger, A. Lamm, Handbook of Fuel Cells: Fundamentals, Technology and Applications, Wiley, New York, 2003.
[2] K. Kordesch, G. Simader, Fuel Cells and Their Applications, Weinheim, VCH, 1996.
[3] R. Rashidi, I. Dincer, G.F. Naterer, P. Berg, J. Power Sources 187 (2009) 509–516.
[4] H. Liu, C. Song, L. Zhang, J. Zhang, H. Wang, D.P. Wilkinson, J. Power Sources 155 (2006) 95–110.
[5] T.D. Jarvi, E.M. Stuve Jr., in: J. Lipkowski, P.N. Ross Jr. (Eds.), Electrocatalysis, Frontiers of Electrochemistry, vol. 4, Wiley-VCH, New York, 1998 (Chapter 3).
[6] S.C. Kelley, G.A. Deluga, W.H. Smyrl, Electrochem. Solid-State Lett. 3 (2000) 407–409.
[7] H.A. Gasteiger, N. Marković, P.N. Ross, E.J. Cairns, J. Phys. Chem. 98 (1994) 617–625.
[8] R. Liu, H. Iddir, Q. Fan, G. Hou, A. Bo, K.L. Ley, E.S. Smotkin, Y. Sung, H. Kim, S. Thomas, A. Wieckowski, J. Phys. Chem. B 104 (2000) 3518–3531.
[9] M. Watanabe, M. Uchida, S. Motoo, J. Electoanal. Chem. 229 (1987) 395–406.
[10] X. Ren, M.S. Wilson, S. Gottesfeld, J. Electrochem. Soc. 143 (1996) L12–L15.
[11] D. Chu, S. Gilman, J. Electrochem. Soc. 143 (1996) 1685–1690.
[12] A.S. Arico, P. Creti, H. Kim, R. Mantegna, N. Giordano, V. Antonucci, J. Electrochem. Soc. 143 (1996) 3950–3959.
[13] K.-W. Park, J.-H. Choi, S.-A. Lee, C. Pak, H. Chang, Y.-E. Sung, J. Catal. 224 (2004) 236–242.
[14] G. García, J.A. Silva-Chong, O. Guillén-Villafuerte, J.L. Rodríguez, E.R. Gonzalez, E. Pastor, Catal. Today 116 (2006) 415–421.
[15] J.R.C. Salgado, E. Antolini, E.R. Gonzalez, Appl. Catal. B: Environ. 57 (2005) 283–290.
[16] E. Antolini, J.R.C. Salgado, A.M. dos Santos, E.R. Gonzalez, Electrochem. Solid-State Lett. 8 (2005) A226–A230.
[17] E. Antolini, J.R.C. Salgado, L.G.R.A. Santos, G. García, E.A. Ticianelli, E. Pastor, E.R. Gonzalez, J. Appl. Electrochem. 36 (2006) 355–362.
[18] M. Gotz, H. Wendt, Electrochim. Acta 43 (1998) 3637–3644.
[19] A.S. Arico, Z. Poltarzewski, H. Kim, A. Morana, N. Giordano, V. Antonucci, J. Power Sources 55 (1995) 159–166.
[20] T. Iwasita, Electrochim. Acta 48 (2002) 289.
[21] T. Frelink, W. Visscher, J.A.R. van Veen, Surf. Sci. 335 (1995) 353–360.
[22] A.L. Dicks, J. Power Sources 156 (2006) 128–141.
[23] C. Lin, T. Wang, F. Ye, Y. Fang, X. Wang, Electrochem. Commun. 10 (2008) 255–258.
[24] R. Gadiou, S.-E. Saadallah, T. Piquero, P. David, J. Parmentier, C. Vix-Guterl, Micropor. Mesopor. Mater. 79 (2005) 121–128.
[25] S. Kim, S.-J. Park, Electrochim. Acta 52 (2007) 3013–3021.
[26] E.R. Gonzalez, E.A. Ticianelli, A.L.N. Pinheiro, J. Perez, Patent Brasileira, INPI-SP No. 00321, 1997.
[27] W.H. Lizcano-Valbuena, V.A. Paganin, E.R. Gonzalez, Electrochim. Acta 47 (2002) 3715–3722.
[28] E.V. Spinace, A.O. Neto, T.R.R. Vasconcelos, M. Linardi, J. Power Sources 137 (2004) 17–23.
[29] W.J. Zhou, S.Q. Song, W.Z. Li, G.Q. Sun, Q. Xin, S. Kontou, K. Poulianitis, P. Tsiakaras, Solid State Ionics 175 (2004) 797–803.
[30] J. Guo, G. Sun, Q. Wnag, G. Wang, Z. Zhou, S. Tang, L. Jiang, B. Zhou, Q. Xin, Carbon 44 (2006) 152–157.
[31] H. Tang, J. Chen, L. Nie, D. Liu, W. Deng, Y. Kuang, S. Yao, J. Colloid Interf. Sci. 269 (2004) 26–31.
[32] E.S. Steigerwalt, G.A. Deluga, D.E. Cliffel, C.M. Lukehart, J. Phys. Chem. B 105 (2001) 8097–8101.
[33] M. Carmo, V.A. Paganin, J.M. Rosolen, E.R. Gonzalez, J. Power Sources 142 (2005) 169–176.

[34] D.-J. Guo, H.-L. Li, J. Power Sources 160 (2006) 44–49.
[35] L. Li, G. Wu, B.-Q. Xu, Carbon 44 (2006) 2973–2983.
[36] M.-C. Tsai, T.-K. Yeh, C.-H. Tsai, Electrochem. Commun. 8 (2006) 1445–1452.
[37] L. Calvillo, M.J. Lázaro, E. García-Bordejé, R. Moliner, P.L. Cabot, I. Esparbé, E. Pastor, J.J. Quintana, J. Power Sources 169 (2007) 59–64.
[38] J.R.C. Salgado, J.J. Quintana, L. Calvillo, M.J. Lázaro, P.L. Cabot, I. Esparbé, E. Pastor, Phys. Chem. Chem. Phys. 10 (2008) 6796–6806.
[39] S.H. Joo, C. Pak, D.J. You, S.-A. Lee, H.I. Lee, J.M. Kim, H. Chang, D. Seung, Electrochim. Acta 52 (2006) 1618–1626.
[40] J. Ding, K.-Y. Chan, J. Ren, F.-S. Xiao, Electrochim. Acta 50 (2005) 3131–3141.
[41] Z. Lei, S. Bai, Y. Xiao, L. Dang, L. An, G. Zhang, Q. Xu, J. Phys. Chem. C 112 (2008) 722–731.
[42] F. Su, J. Zeng, X. Bao, Y. Yu, J.Y. Lee, X.S. Zhao, Chem. Mater. 17 (2005) 3960–3967.
[43] J.-H. Nam, Y.-Y. Jang, Y.-U. Kwon, J.-D. Nam, Electrochem. Commun. 6 (2004) 737–741.
[44] S.H. Joo, K. Kwon, D.J. You, C. Pak, H. Chang, J.M. Kim. Electrochim. Acta (2008), doi:10.1016/j.electacta.2009.05.022.
[45] Z.-P. Sun, X.-G. Zhang, Y.-Y. Liang, H.-L. Li. J. Electroanal. Chem. (2009), doi:10.1016/j.jelechem.2009.04.013.
[46] A.E. Aksoylu, M. Madalena, A. Freitas, M.F.R. Pereira, J.L. Figueiredo, Carbon 39 (2001) 175–185.
[47] M.C. Román-Martínez, D. Cazorla-Amorós, A. Linares-Solano, C. Salinas-Martínez de Lecea, Carbon 33 (1995) 3–13.
[48] A. Sepúlveda-Escribano, F. Coloma, F. Rodríguez-Reinoso, Appl. Catal. A: Gen. 173 (1998) 247–257.
[49] C. Prado-Burguete, A. Linares-Solano, F. Rodríguez-Reinoso, C. Salinas-Martínez de Lecea, J. Catal. 115 (1989) 98–106.
[50] M.A. Fraga, E. Jordao, M.J. Mendes, M.M.A. Freitas, J.L. Faria, J.L. Figueiredo, J. Catal. 209 (2002) 355–364.
[51] A. Guerrero-Ruiz, P. Badenes, I. Rodríguez-Ramos, Appl. Catal. A: Gen. 173 (1998) 313–321.
[52] M.J. Lázaro, L. Calvillo, E. García-Bordejé, R. Moliner, R. Juan, C.R. Ruiz, Micropor. Mesopor. Mater. 103 (2007) 158–165.
[53] B.E. Warren, X-ray Diffraction, Addison-Wesley, Reading, 1969.
[54] W. Li, W. Zhou, H. Li, Z. Zhou, B. Zhou, G. Sun, Q. Xin, Electrochim. Acta 49 (2004) 1045–1055.
[55] Y.P. Mascarenhas, J.M.V. Pinheiro, Programa para Cálculo de Parâmetro de Rede pelo Método de Mínimos Quadrados, Salvador, SBPC, 1985.
[56] L. dos Santos, F. Colmati, E.R. Gonzalez, J. Power Sources 159 (2006) 869–877.
[57] C.A. Bessel, K. Laubernds, N.M. Rodríguez, R.T.K. Baker, J. Phys. Chem. B 105 (2001) 1115–1118.
[58] P. Serp, M. Corrias, P. Kalck, Appl. Catal. A: Gen. 253 (2003) 337–358.
[59] H.A. Gasteiger, N. Marković, P.N. Ross, E.J. Cairns, J. Phys. Chem. 97 (1993) 12020–12029.
[60] T. Iwasita, Electrochim. Acta 47 (2002) 3663–3674.
[61] T. Frelink, W. Visscher, J.A.R. van Veen, Langmuir 12 (1996) 3702–3708.
[62] P. Sivakumar, V. Tricoli, Electrochim. Acta 51 (2006) 1235–12343.
[63] H.A. Gasteiger, N. Markivic, P.N. Ross, E.J. Cairns, J. Electrochem. Soc. 141 (1994) 1795–1803.
[64] J. Jiang, A. Kucernak, J. Electroanal. Chem. 543 (2003) 187–199.
[65] V. Raghuveer, A. Manthiram, J. Electrochem. Soc. 152 (2005) A1504–A1510.
[66] D.B. Sepa, in: B.E. Conway, R.E. White, J.O'M. Bockris (Eds.), Modern Aspects of Electrochemistry, vol. 129, Plenum Press, New York, 1996, p. 1.
[67] G. Tremillosi-Filho, H. Kim, W. Chrzanowski, A. Wieckowski, B. Grzybowska, P. Kulesza., J. Electroanal. Chem. 467 (1999) 143–156.
[68] T.H. Madden, N. Arvindan, E.M. Stuve, J. Electrochem. Soc. 150 (2003) E1–E10.
[69] J.l. Cohen, D.J. Volpe, H.D. Abruña, Phys. Chem. Chem. Phys. 9 (2007) 49–77.